Technical University of Denmark

DTU

Tissue Harmonic Synthetic Aperture Ultrasound Imaging

Hemmsen, Martin Christian; Rasmussen, Joachim; Jensen, Jørgen Arendt

Document Version
Early version, also known as pre-print

Link back to DTU Orbit

DTU Library
Technical Information Center of Denmark

Tissue Harmonic Synthetic Aperture Ultrasound Imaging

Martin Christian Hemmsen,[a)] Joachim Hee Rasmussen, and Jørgen Arendt Jensen

Center for Fast Ultrasound Imaging,

Department of Electrical Engineering,

Technical University of Denmark,

Ørsteds Plads,

Bldg. 349,

DK-2800 Kgs. Lyngby,

Denmark

(Dated: July 4, 2014)

Abstract

Synthetic aperture sequential beamforming (SASB) and tissue harmonic imaging (THI) are combined to improve the image quality of medical ultrasound imaging. The technique is evaluated in a comparative study against dynamic receive focusing (DRF). The objective is to investigate if SASB combined with THI improves the image quality compared to DRF-THI. The major benefit of SASB is a reduced bandwidth between the probe and processing unit. A BK Medical 2202 Ultraview ultrasound scanner was used to acquire beamformed RF data for offline evaluation. The acquisition was made interleaved between methods, and data were recorded with and without pulse inversion for tissue harmonic imaging. Data were acquired using a Sound Technology 192 element convex array transducer from both a wire phantom and a tissue mimicking phantom to investigate spatial resolution and penetration. *In-vivo* scans were also performed for a visual comparison. The spatial resolution for SASB-THI is on average 19% better than DRI-THI, and the investigation of penetration showed equally good signal-to-noise ratio. *In-vivo* B-mode scans were made and compared. The comparison showed that SASB-THI reduces the artefact and noise interference and improves image contrast and spatial resolution.

I. INTRODUCTION

Tissue harmonic imaging (THI) can be used in ultrasound investigations to image difficult regions of the human body and to generally improve the image quality. Synthetic aperture imaging (SAI) is a focusing technique that generates images focused in both transmit and receive. The scope of this study is to investigate if synthetic aperture sequential beamforming (SASB) can be combined with tissue harmonic imaging for improved image quality.

THI benefits from improved spatial resolution, lower side lobe levels, less reverberation, and a narrower beam profile compared to conventional B-mode imaging[1–3]. The narrow beam profile of THI is used in many thoracic investigations to image tissues such as the heart valves that lie close to e.g. air filled regions in the lungs or bone in the rib cage, which would otherwise interfere and obscure the final image. The higher spatial resolution of THI is also used in many abdominal investigations to image small objects in e.g. the gall bladder or kidneys. In many abdominal scans THI is used to penetrate fatty tissues that surround the area of interest. In the recent years, the use of THI is increased and has in many cases become the default setting on scanners when performing abdominal scans.

The concept in THI is to transmit a waveform with a fundamental frequency and receive and image the response at a harmonic frequency. Inherent to THI is that only a fraction of the transmitted fundamental waveform energy is transformed into harmonics. The magnitude of the harmonic waveform is dependent on the magnitude of the emitted acoustic field. It is therefore important in THI to emit a field intense enough to ensure good development of harmonic waveforms.

———

[a)]Author to whom correspondence should be addressed. Electronic mail: `mah@elektro.dtu.dk`

Tissue harmonic imaging has been combined with a variety of focusing techniques, including dynamic receive focusing (DRF) to further improve image quality. Synthetic aperture imaging is a focusing technique that generates focused images in both transmit and receive[4–6]. In the synthetic aperture focusing technique[7] an active aperture of a single element is used in transmit and receive. For every position of the active aperture, a low resolution image is constructed and in the end all low resolution images are combined to create one high resolution image. Naturally, because only one element is used, the signal-to-noise ratio (SNR) is very poor using this technique. Also, because a full low resolution image has to be beamformed for every line, the computational load of beamforming is extensive. Several SAI techniques have been suggested to improve SNR, including the use of multi-element transmit and receive aperture as suggested by Karaman et al.[8]. Here a group of elements are used in transmit to increase the SNR. By focusing multiple elements in a single point in transmit, a virtual source is created as first described by Passmann and Ermert[9] and further investigated by Frazier and O'Brien[10], Nikolov and Jensen[11,12], Gammelmark and Jensen[13], and Bae and Jeong[14].

The use of several electronically focused elements in the aperture for generating virtual sources causes the emitted ultrasound energy field to increase in intensity. This causes development of higher harmonic ultrasound waveforms. Depending on the magnitude of the emitted field, SAI could be combined with THI by isolating and imaging the second harmonic waveform of the received response. Such a technique has been suggested by Li et al.[15] for a single element transducer and by Bae et al.[16] for a multi element array transducer. In both studies, however, the computational load required to produce SAI is still a major drawback.

Synthetic Aperture Sequential Beamforming (SASB) is a technique that utilizes a two step beamformer to significantly reduce computational processing load compared to traditional SAI[17–19]. It has earlier been clinically evaluated to perform at least as

good as conventional dynamic receive focusing[20]. In SASB, a set of scan lines are first obtained and beamformed using a fixed focus in both transmit and receive. Secondly, the image data are beamformed using the fixed focus points as virtual sources to obtain the final synthetic aperture image. The advantage of SASB, besides the reduction in computational load, is that the lateral resolution remains higher and more uniform over depth compared to regular dynamic receive focusing (DRF)[19]. The use of virtual sources in SASB has been shown to create an acoustic field intense enough to generate harmonics[21,22].

By combining THI with a SAI technique such as SASB, which is capable of generating harmonics for THI, the final image could potentially be improved by both techniques. The improvements could be increased spatial resolution, reduced reverberation artefacts, reduced side lobe levels, and a narrower beam profile.

This paper presents the combined method of THI using pulse inversion and SASB beamforming. The method is evaluated using a BK Medical 2202 Ultraview scanner and a Sound Technology 192 element convex array transducer. Spatial resolution and penetration depth is evaluated in a comparative study between DRF and SASB. A comparison is also made on clinically acquired *in-vivo* data.

II. THEORY

A. Pulse Inversion

In THI, it is often the purpose to image the second harmonic frequency instead of the transmitted fundamental frequency. As a transmitted ultrasound waveform propagates in a medium, the waveform gets distorted due to the non-linearity of the signal speed in the propagating waveform[23–26]. The speed at which the waveform travels (the speed of sound) depends on the instantaneous acoustic pressure within the waveform. Because there is a pressure difference between the high pressure peaks and the relatively low pressure troughs

of the waveform, different parts of the waveform travels at different speeds[27]. This causes the high pressure peaks to travel a higher speed of sound than the relatively low pressure troughs. As the waveform gets continuously distorted, higher harmonics are generated in the waveform. The strength of these harmonics is dependent on the acoustic pressure of the emitted ultrasound field. It is therefore important to emit a field intense enough to ensure good development of harmonic waveforms.

In THI it is also important to ensure good separation of the desired harmonic frequency from unwanted neighbouring frequencies. Several techniques exist to separate and enhance harmonic frequencies such as matched filtering, power modulation, and pulse inversion (PI)[28–30]. In PI, two identical but phase shifted pulses (0° phase shifted and 180° phase shifted pulse) are transmitted interleaved. Under the assumption that there has been no motion in the medium in the time between the two waveforms were transmitted, differences in the responses are purely a result from how the waveforms were distorted by the medium. For the received pair of responses, a 180° phase shift between the two waveforms can be detected at the fundamental frequency. However, for the 2nd and 3rd harmonic frequencies, a corresponding 360° and 540° phase shift can be detected in the pair of waveforms respectively[31,32]. If the two responses are summed, all signals that are perfectly in phase will double in signal strength, while all signals that have opposite phases will cancel out. To suppress the odd order harmonics then, each pair (inverted and non-inverted waveform) of the received responses are summed. The harmonic frequencies that are in phase (all even harmonics) will double in amplitude, while out of phase harmonic frequencies (all odd harmonics) will cancel out.

B. Synthetic Aperture Sequential Beamforming

Synthetic aperture sequential beamforming (SASB) is a SAI technique, which significantly reduces the computational load and number of receiving data channels between the probe and the processing unit compared to SAI[20,33]. The transmitted acoustic energy is

sufficient to produce harmonic components for THI as a focused emission is used[21]. In the initial stage of the SASB method, a first stage beamformer operates on the signals received by the transducer array. The emission sequence scans a focused emission across the volume being imaged, and the beamformer applies delay-and-sum beamforming with a fixed delay for each transducer element to create a fixed focus scan line. The delay configuration is identical in both transmit and receive. Fig. 1 illustrates the wave propagation path and how to determine the time-of-flight calculation for the first stage beamformer.
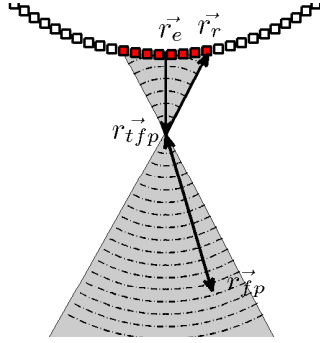

Figure 1. (Color online) Wave propagation path - first stage. The dashed lines indicate the propagating waves for a single multi element emission. The white squares indicate the individual transducer elements of a 1D transducer, and the red squares the active elements. The wave propagation path is shown as a solid line with arrow head to indicate direction. $\vec{r}_{fp}$ is the receive sample focus point, $\vec{r}_{tfp}$ is the virtual source position, $\vec{r}_e$ is the scan line reference position, and $\vec{r}_r$ is the position of the receiving element.

The second stage beamformer takes the output of the first stage as input. The focal point from the first stage beamformer is considered a virtual source, while the samples on the scan line are considered the signal received by a virtual receive element co-located with the virtual source. Each point in the focused scan line contains information from a set of spatial positions limited by the opening angle of the virtual source. A single image point is therefore potentially represented in multiple first stage focused scan lines. The second stage beamformer creates a set of image points by combining information from the first stage focused scan lines that contain information from the spatial position of the image

7

point[34]. Fig. 2 illustrates the wave propagation path used in the second stage beamformer to beamform the output from the first stage beamformer.
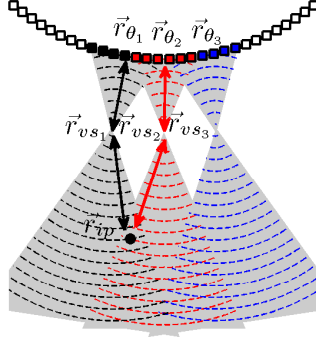

Figure 2. (Color online) Wave propagation path - second stage. The dashed lines indicate the propagating waves for three multi element emissions. The squares indicate the individual transducer elements of a 1D transducer. The black dot indicates a specific image point. The wave propagation path is shown as a solid line with arrow head, to indicate direction. Note that the third emission shown in blue does not contribute to the image point as it contains no information about the spatial position of the image point due to the limited opening angle. $\vec{r}_{ip}$ is the position of a image point, $\vec{r}_{vs}$ is the position of the virtual source, and $\vec{r}_{\theta}$ is the first stage scan line reference position.

III. METHODS

To perform the comparative study between DRF and SASB, several experiments were performed and data were acquired and processed offline. The measurements were performed using a data acquisition system consisting of a 2202 UltraView scanner (BK Medical, Herlev, Denmark) equipped with a research interface connected to a standard PC[35,36]. The system enables acquisition of several seconds of real-time beamformed data, and it is remotely controlled through a developed Matlab Software Development Kit (MathWorks Inc., Natick, Mass., USA). The system allows for user defined scan sequences, and is capable of performing

both synthetic aperture imaging and tissue harmonic imaging[21,37]. In the following evaluations, measurements are performed with identical transmit settings for both techniques to perform a fair comparisons. This includes identical excitation waveform, transmit amplitude, transmit apodization, Time-gain-compensation, and field-of-view. Data frames were acquired interleaved to allow images of the same *in-vivo* view to be obtained, enabling direct comparison of the methods. The depth of each scan was set to 14.6 cm and the interleaved frame rate was set to 5 frames/s, i.e., 5 conventional and 5 SASB frames/s. The excitation waveform is a 2 cycle 2.14 MHz sinusoid. Each data frame consist of 269 scan lines, acquired using 64 elements in transmit. The transmit focus were specified to 70 mm. In the following experiments an abdominal 3.5 MHz probe with a room-temperature vulcanization (RTV) lens, 3.5CL192-3ML (Sound Technology Inc., 1363 South Atherton St., State College, PA 16801, USA) transducer was used.

A. Data Processing

The DRF data were beamformed by the scanner using a dynamically expanding receive aperture (F# :0.8) and a Gaussian ($\alpha = 0.4$) window with raised edge levels. The first stage beamformer in the SASB algorithm were implemented on the scanner using a fixed receive focus at 70 mm using a fixed aperture (F# :2) and a Gaussian ($\alpha = 0.4$) apodization window with raised edge levels. The acquired data were subsequently extracted in Matlab and the second stage beamforming were performed using the beamformation toolbox BFT3[38]. The SASB algorithm was specified to produce the same spatial samples as created by the DRF algorithm for direct comparison. Dynamic apodization was applied in the second stage beamformer using a Gaussian window ($\alpha = 0.4$). The THI images were created offline by adding the respective scan lines in accordance with the pulse inversion technique. In the SASB algorithm the first stage beamformed scan lines were added prior to second stage beamforming.

B. In-vivo comparison

Prior to conducting the in-vivo experiment, the acoustic outputs of the ultrasound scanner were measured for the imaging modes under investigation. The measured intensities need to satisfy pre-amendments upper limits regulated by the United States Food and Drug Administration (FDA, 1997), which have been introduced as safety guides to avoid damage to the tissue and pain to the patient. These limits concern the mechanical index, $MI \leq 1.9$, the derated spatial-peak-pulse-average intensity, $I_{sppa} \leq 190 \ W/cm^2$, and the derated spatial-peak-temporal-average intensity $I_{spta} \leq 720 \ mW/cm^2$ (FDA, 1997). The acoustic outputs were measured in a water tank using a high precision 3-dimensional position system and a HGL0400 hydrophone (Onda, Sunnyvale, CA, USA) by following the guidelines given by the American Institute of Ultrasound in Medicine (AIUM, 1998). The levels obtained for I_{spta} is 16.2 mW/cm^2, I_{sppa} is 81.2 W/cm^2 and MI is 0.9. These values are considerably lower than the FDA limits and in-vivo scanning is therefore safe using the present imaging modes.

IV. RESULTS

Harmonic imaging relies on the fact that the speed of sound depends on the acoustic pressure and a cumulative distortion in the propagating waveform. As the waveform distorts in the time domain, it generate new frequency components in the frequency domain. These components are harmonically related and the distortion increases as the source intensity increases and as the wave propagates. The cumulation of non-linearly distortion is the formation of vertical discontinuity in the waveform, known as shocks. At a shock parameter value of $\sigma = 3$, a mature shock is formed and the fundamental has lost 6 dB to harmonic build-up[23].

A. Harmonic Imaging

To enhance the second harmonic and suppress the fundamental frequency, pulse inversion and bandpass filtering is applied. The pulse inversion technique can potentially double the amplitude of the second harmonic, corresponding to a 6 dB gain. To investigate the harmonic build-up, first stage beamformed data are acquired from a water phantom with a set of metal wires. Fig. 3 shows the two received pulse-echo responses of the 5th wire in the water phantom (approximately 5 cm from the focus point). Here, the pulse inversion of the transmitted pulses are clearly seen. Note, that the zero-crossing of both responses almost coincide. In the right part of Fig. 3 the response after pulse summation is shown. It is this response, that contains the enhanced second harmonic and is used in THI.

A Received time responses   **B** Summed time response
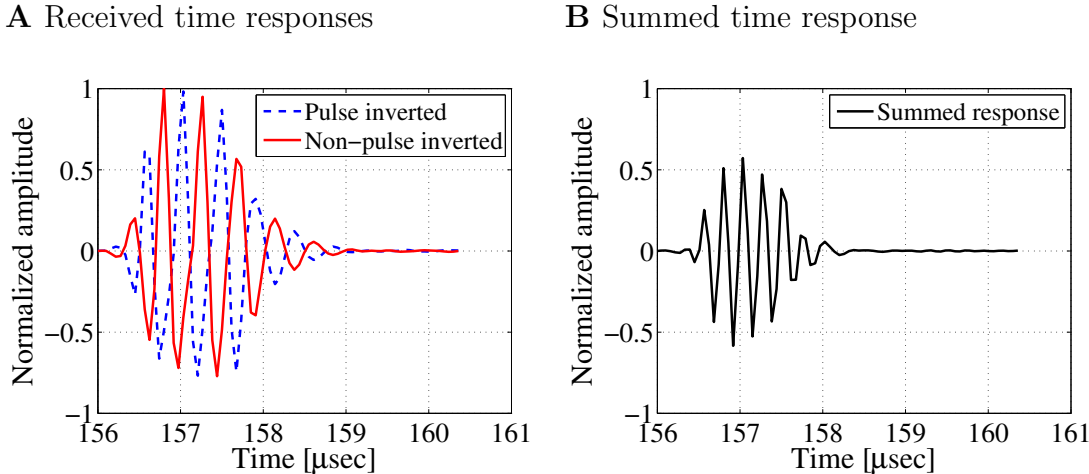
Figure 3. (Color online) The two received responses from the scan line going through a wire are shown in subfigure A. Note the 180° phase shift between the two received responses. The summed response is shown in subfigure B. All waveforms have been normalized to the maximum amplitude of the pulse inverted response.

From the magnitude spectrum of the received responses, shown in Fig. 4, the amplitude of the second harmonic is measured to be -11.69 and -13.91 dB for the inverted and non-inverted waveform. The difference in spectrum is because of the non-linearities of the

transducer and front-end of the scanner. After pulse summation the magnitude of the second harmonic is -6.87 dB, resulting in a gain between 4.8 and 7 dB. This shows that not only are the harmonics being build-up, they are also enhanced using pulse inversion.
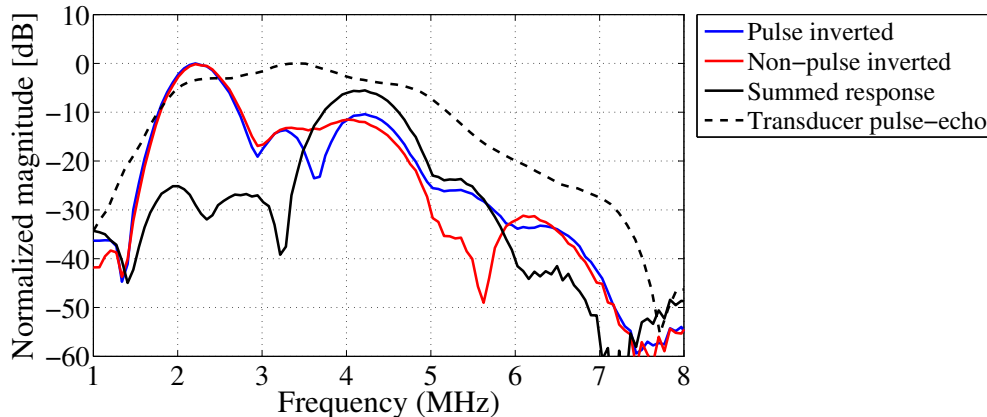

Figure 4. (Color online) Magnitude spectrum of received pulse echo responses and pulse echo transfer function of the transducer.

B. Spatial resolution

To evaluate the spatial resolution, data were acquired from a water-filled wire phantom. B-mode images for DRF, SASB, DRF-THI, and SASB-THI were produced from the collection of data and are shown in Fig. 5.

From the B-mode images the -6 dB lateral resolution (FWHM) and -20 dB lateral resolution (FWTM) were measured for each visible wire. Fig. 6A shows the measured FWHM as function of depth. As seen from the figure, SASB and SASB-THI generally produces lower FWHM values than DRF and DRF-THI respectively. As expected the FWHM using THI is lower than that of the fundamental frequency. In Fig. 6B the measured FWTM values are shown. SASB produces a worse FWTM than DRF, but SASB-THI is better than DRF-THI.

Fig. 7 shows a color encoded zoom of of the B-mode images of the wire located at 95 mm depth. Note how the point spread function created using SASB-THI is more narrow

12

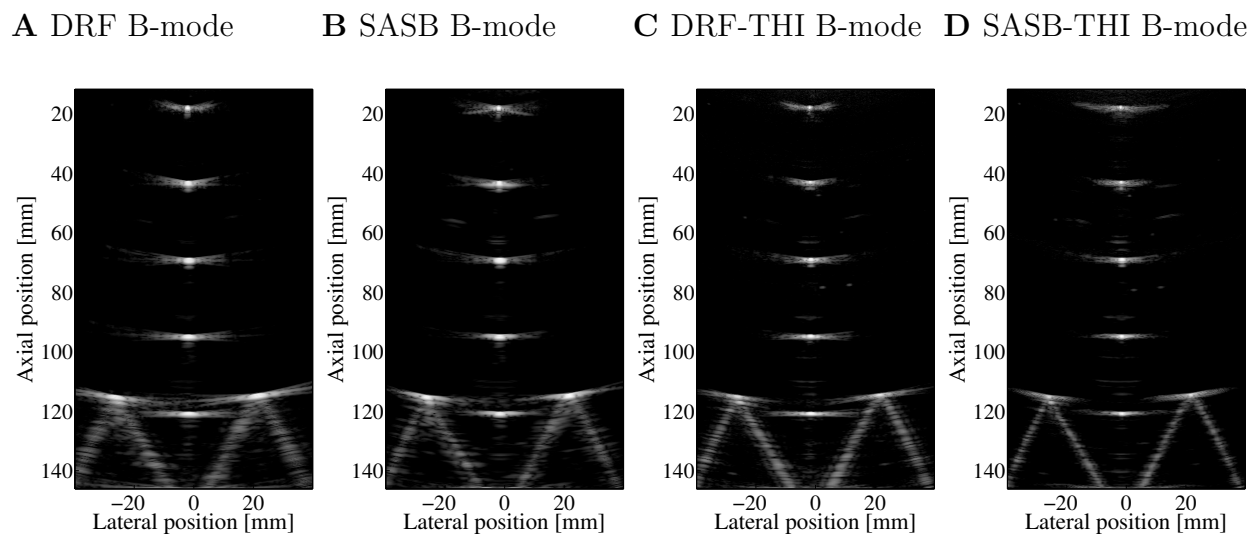**A** DRF B-mode   **B** SASB B-mode   **C** DRF-THI B-mode **D** SASB-THI B-mode

Figure 5. B-mode images of a wire phantom with 5 metal wires centred along the middle of the image and the pyramidal shaped damping material at the bottom.

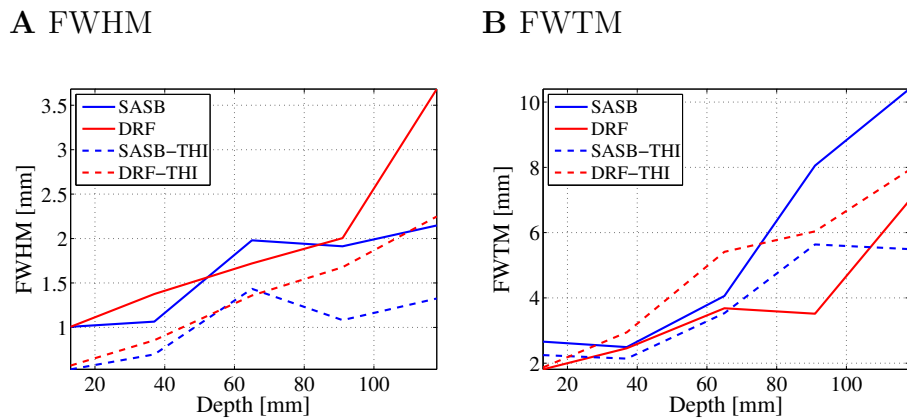**A** FWHM   **B** FWTM

Figure 6. (Color online) Measured (A) -6 dB lateral resolution (FWHM) and (B) -20 dB lateral resolution (FWTM).

and compact compared to the one created using DRF-THI.

C. Penetration

A major problem with defocused transmit SA imaging is the limited penetration depth. The problem can be solved by combining several elements for transmission and using longer

A DRF PSF **B** SASB PSF **C** DRF-THI PSF **D** SASB-THI PSF
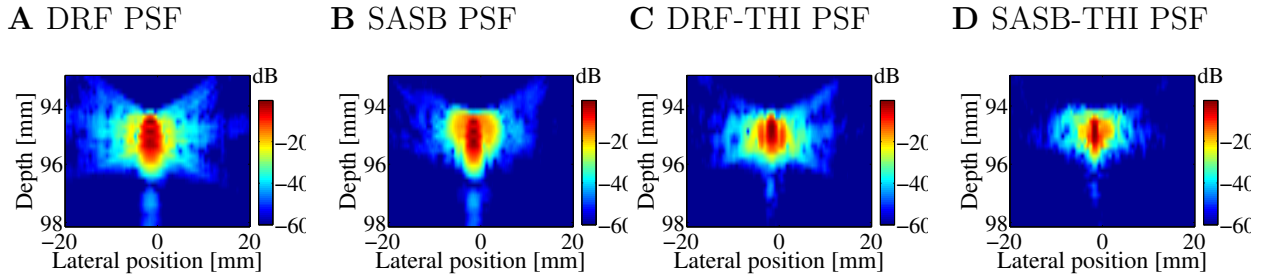
Figure 7. (Color online) Zoomed B-mode image for the wire at 95 mm depth using DRF, SASB, DRF-THI, and SASB-THI.

or coded waveforms emitting more energy[8,39]. Another way to solve the problem is to move the virtual source in-front of the transducer using focused transmissions[9,10,40]. In this study the virtual sources are positioned in-front of the transducer at 70mm depth and coincide with the transmit focus of DRF. To evaluate the penetration depth, data were acquired from a tissue mimicking phantom which has an attenuation of 0.5 dB/(MHz·cm). A total of 50 DRF and SASB frames were acquired and beamformed. A measurement of the signal-to-noise ratio (SNR) was performed based on the mean signal energy and noise energy found from the collection of data. Fig. 8 illustrates the SNR as function of depth, and it is seen that SASB-THI and DRF-THI produces equally good signal-to-noise ratios.
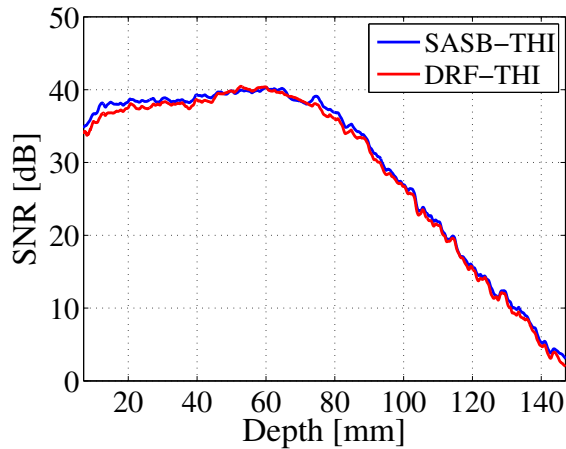
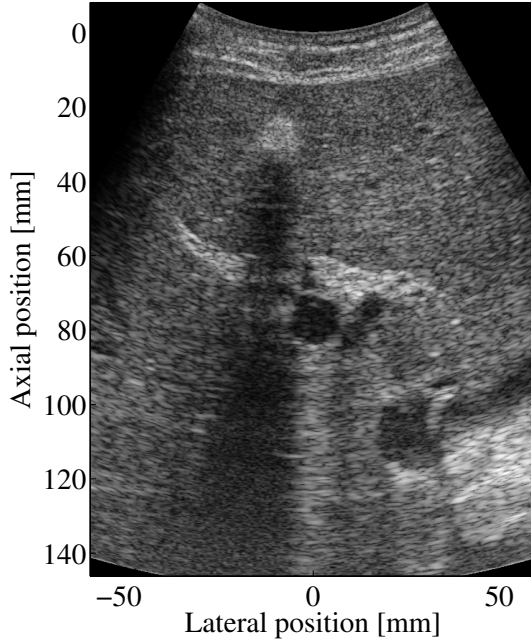Figure 8. (Color online) Signal-to-noise ratio for SASB-THI and DRF-THI.

D. Clinical results

From the previous sections, it can be seen that SASB imaging has several advantages compared to conventional ultrasound imaging. It is, however, not clear whether these advantages also translate to the clinical image, and it is, therefore, important to conduct a pre-clinical trial to realistically study the performance. This has been done where the ultrasound system was programmed to acquire both data for the conventional image and the SASB image. The sequences were acquired interleaved to have the same region of interest, transducer, and transmit characteristic profile. The only change is, thus, the beamforming method. An example of clinical images are shown in Fig. 9 and shows the right liver lobe. Close to the liver capsule is a 1.5 cm large focal lesion with shadowing. The portal vein is seen below with enhancement. The lesion resembles a hemoangioma or single metastasis. A subsequent biopsy has confirmed the suspicion of metastasis. The two images are very similar in appearance, however, minute differences can be spotted on close inspections. For the SASB-THI image, the shadowing feature is less dominant and the width is smaller compared with the DRF-THI image.

V. CONCLUSION

Traditionally, defocused transmits are applied in synthetic imaging. However, since this would decrease the harmonic signal strength, focused transmits needs to be applied. In this paper a method for tissue harmonic synthetic aperture imaging has been suggested. SASB utilizes a focused transmit and is capable of producing harmonics for THI. The advantage of SASB compared to other suggested synthetic aperture THI techniques is that the data transfer between the transducer and the processing unit is limited to 30 MB/sec. In the previously suggested synthetic aperture THI technique by Bae et al.[16], data from all elements from every emission are stored in receive. This data is then used to beamform a whole low resolution image for every image line in the high resolution image. In SASB, only the data output from the first stage beamformer is stored from each emission. This image line data is

A DRF-THI - *In-vivo* imaging   **B** SASB-THI - *In-vivo* imaging
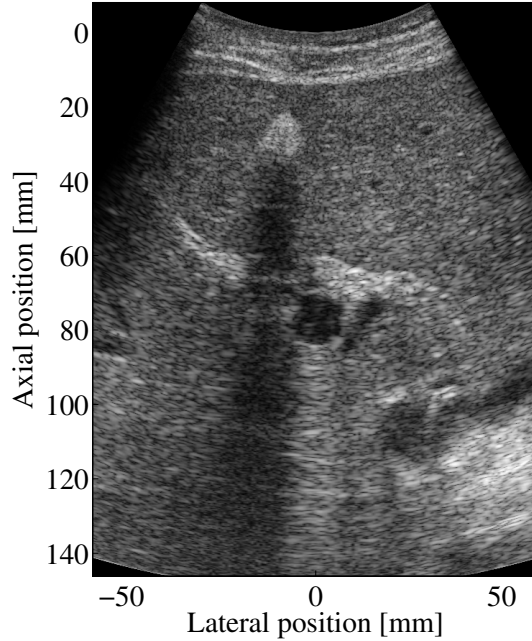

Figure 9. *In-vivo* image of the right liver lobe. Close to the liver capsule is a 1.5 cm large focal lesion with shadowing. The portal vein is seen below with enhancement. Images are shown with 60 dB dynamic range. Acquisitions are made using DRF-THI and SASB-THI simultaneously on the BK 2202 UltraView scanner.

then processed by the second stage beamformer, which has the complexity of a traditional dynamic receive beamformer. The reduction in data storage is equivalent to the number of channels in the system. For a 64 channel system, the reduction in data bandwidth is therefore 64 times for SASB compared with traditional SAI techniques. The SASB technique was implemeted using a BK Medical UltraView scanner and a stand-alone PC. Investigations show that it is possible to compliment synthetic aperture sequential beamforming with tissue harmonic imaging for improved image quality. The investigation of spatial resolution showed that SASB-THI performs better than DRI-THI, and the investigation of penetration showed equally good signal-to-noise ratio. *In-vivo* B-mode scans were made and compared with conventional imaging. The images showed minute improvements in resolution, delineation,

and contrast in the SASB-THI image, but needs further evaluation in a larger clinical trial.

Acknowledgment

References

[1] B. Ward, A. C. Baker, and V. F. Humphrey, "Nonlinear propagation applied to the improvement of resolution in diagnostoc medical ultrasound", J. Acoust. Soc. Am. **101**, 143–154 (1997).

[2] T. Christopher, "Finite amplitude distortion-based inhomogeneous pulse echo ultrasonic imaging", IEEE Trans. Ultrason., Ferroelec., Freq. Contr. **44**, 125–139 (1997).

[3] M. A. Averkiou and M. F. Hamilton, "Measurements of harmonic generations in a focused finite-amplitude sound beam", J. Acoust. Soc. Am. **98**, 3439–3442 (1995).

[4] L. J. Cutrona, W. E. Vivian, E. N. Leith, and G. O. Hall, "A high resolution radar combat-surveillance system", IRE Trans. Mil. Elect. **MIL-5**, 127–131 (1961).

[5] C. W. Sherwin, J. P. Ruina, and D. Rawcliffe, "Some early developements in synthetic aperture radar systems", IRE Trans. Mil. Elect. **MIL-6**, 111–115 (1962).

[6] J. C. Curlander and R. N. McDonough, *Synthetic Aperture Radar: Systems and Signal Processing* (John Wiley & Sons, Inc.) (1991) (535).

[7] R. Thomson, "Transverse and longitudinal resolution of the synthetic aperture focusing technique", Ultrasonics **22**, 9–15 (1984).

[8] M. Karaman, P. C. Li, and M. O'Donnell, "Synthetic aperture imaging for small scale systems", IEEE Trans. Ultrason., Ferroelec., Freq. Contr. **42**, 429–442 (1995).

[9] C. Passmann and H. Ermert, "A 100-MHz ultrasound imaging system for dermatologic and ophthalmologic diagnostics", IEEE Trans. Ultrason., Ferroelec., Freq. Contr. **43**, 545–552 (1996).

[10] C. H. Frazier and W. D. O'Brien, "Synthetic aperture techniques with a virtual source element", IEEE Trans. Ultrason., Ferroelec., Freq. Contr. **45**, 196–207 (1998).

[11] S. I. Nikolov and J. A. Jensen, "Virtual ultrasound sources in high-resolution ultrasound imaging", in *Proc. SPIE - Progress in biomedical optics and imaging*, volume 3, 395–405 (2002).

[12] S. I. Nikolov and J. A. Jensen, "3D synthetic aperture imaging using a virtual source element in the elevation plane", in *Proc. IEEE Ultrason. Symp.*, volume 2, 1743–1747 (2000).

[13] K. L. Gammelmark and J. A. Jensen, "Multielement synthetic transmit aperture imaging using temporal encoding", IEEE Trans. Med. Imag. **22**, 552–563 (2003).

[14] M. H. Bae and M. K. Jeong, "A study of synthetic-aperture imaging with virtual source elements in B-mode ultrasound imaging systems", in *IEEE Trans. Ultrason., Ferroelec., Freq. Contr.*, volume 47, 1510–1519 (2000).

[15] M. L. Li, W. J. Guan, and P. C. Li, "Improved synthetic aperture focusing technique with application in high-frequency ultrasound imaging", IEEE Trans. Ultrason., Ferroelec., Freq. Contr. **51**, 63–70 (2004).

[16] M. Bae, H. Lee, S. B. Park, R. Yoon, M. H. Jeong, D. G. Kim, M. Jeong, and Y. Kim, "A new ultrasonic synthetic aperture tissue harmonic imaging system", in *Proc. IEEE Ultrason. Symp.*, 1258–1261 (2008).

[17] J. Kortbek, J. A. Jensen, and K. L. Gammelmark, "Sequential beamforming for synthetic aperture imaging", Ultrasonics **53**, 1–16 (2013).

[18] J. A. Jensen, J. Kortbek, S. I. Nikolov, M. C. Hemmsen, and B. Tomov, "Implementation of synthetic aperture imaging in medical ultrasound: The dual stage beamformer approach", in *EUSAR*, 434–437 (2010).

[19] M. C. Hemmsen, J. M. Hansen, and J. A. Jensen, "Synthetic Aperture Sequential Beamformation applied to medical imaging using a multi element convex array transducer", in *EUSAR*, 34–37 (2012).

[20] M. Hemmsen, P. M. Hansen, T. Lange, J. M. Hansen, K. L. Hansen, M. B. Nielsen,

and J. A. Jensen, "In vivo evaluation of synthetic aperture sequential beamforming", Ultrasound Med. Biol. **38**, 708–716 (2012).

[21] Y. Du, J. Rasmussen, H. Jensen, and J. A. Jensen, "Second harmonic imaging using synthetic aperture sequential beamforming", in *Proc. IEEE Ultrason. Symp.*, 2261–2264 (2011).

[22] J. H. Rasmussen, M. C. Hemmsen, S. S. Madsen, P. M. Hansen, M. B. Nielsen, and J. A. Jensen, "Implementation of tissue harmonic synthetic aperture imaging on a commercial ultrasound system", in *Proc. IEEE Ultrason. Symp.*, 121–125 (2012).

[23] T. G. Muir and E. L. Carstensen, "Prediction of nonlinear acoustic effects at biomedical frequencies and intensities", Ultrasound Med. Biol. **1980**, 345–357 (1980).

[24] F. A. Duck, "Nonlinear acoustics in diagnostic ultrasound", Ultrasound Med. Biol. **28**, 1–18 (2002).

[25] J. A. Shooter, T. G. Muir, and D. T. Blackstock, "Acoustic saturation of spherical waves in water", J. Acoust. Soc. Am. **55**, 54–62 (1974).

[26] H. C. Starritt, M. A. Perkins, F. A. Duck, and V. F. Humphrey, "Evidence for ultrasonic finite-amplitude distortion in muscle using medical equipment", J. Acoust. Soc. Am. **77**, 302–306 (1985).

[27] R. T. Beyer, *Nonlinear Acoustics* (Department of the Navy) (1974) (452).

[28] C. S. Chapman and J. C. Lazenby, "Ultrasound imaging system employing phase inversion subtraction to enhance the image", US Patent 5632277 (1997).

[29] D. H. Simpson, C. T. Chin, and P. N. Burns, "Pulse inversion Doppler: a new method for detecting nonlinear echoes from microbubble contrast agents", IEEE Trans. Ultrason., Ferroelec., Freq. Contr. **46**, 372–382 (1999).

[30] X. A. A. M. Verbeek, L. A. F. Ledoux, J. M. Willigers, P. J. Brands, and A. P. G. Hoeks, "Experimental investigation of the pulse inversion technique for imaging ultrasound contrast agents", J. Acoust. Soc. Am. **107**, 2281–2290 (2000).

[31] J. A. Jensen, "Medical ultrasound imaging", Prog. Biophys. Mol. Biol. **93**, 153–165 (2007).

[32] M. A. Averkiou, "Tissue harmonic imaging", in *Proc. IEEE Ultrason. Symp.*, volume 2, 1563–1572 (2000).

[33] J. Kortbek, J. A. Jensen, and K. L. Gammelmark, "Synthetic aperture sequential beamforming", in *Proc. IEEE Ultrason. Symp.*, 966–969 (2008).

[34] M. C. Hemmsen, M. F. Rasmussen, M. B. Stuart, and J. A. Jensen, "Simulation study of real time 3d synthetic aperture sequential beamforming for ultrasound imaging", in *Proc. SPIE Med. Imag.*, volume 9040, 90401K1–9 (2014).

[35] M. C. Hemmsen, M. M. Petersen, S. I. Nikolov, M. B., Nielsen, and J. A. Jensen, "Ultrasound image quality assessment: A framework for evaluation of clinical image quality", in *Proc. SPIE Med. Imag.*, volume 76291, 76290C1–12 (Medical Imaging 2010: Ultrasonic Imaging, Tomography, and Therapy) (2010).

[36] M. C. Hemmsen, J. M. Hansen, and J. A. Jensen, "Synthetic Aperture Sequential Beamformation applied to medical imaging using a multi element convex array transducer", in *Proc. IEEE Ultrason. Symp.*, 34–37 (2011).

[37] J. Rasmussen, Y. Du, and J. A. Jensen, "Non-linear imaging using an experimantal synthetic aperture real time ultrasound scanner", IFMBE Proceedings **34**, 101–104 (2011).

[38] J. M. Hansen, M. C. Hemmsen, and J. A. Jensen, "An object-oriented multi-threaded software beamformation toolbox", in *Proc. SPIE Med. Imag.*, volume 7968, 79680Y 1–9 (2011), URL `http://dx.doi.org/10.1117/12.878178`.

[39] M. O'Donnell, "Coded excitation system for improving the penetration of real-time phased-array imaging systems", IEEE Trans. Ultrason., Ferroelec., Freq. Contr. **39**, 341–351 (1992).

[40] C. Passmann and H. Ermert, "Adaptive 150 MHz ultasound imaging of the skin and the eye using an optimal combination of short pulse mode and pulse compression mode", in *Proc. IEEE Ultrason. Symp.*, 1291–1294 (1995).

List of Figures